Ocean Sci. Discuss., 6, 2911–2937, 2009
www.ocean-sci-discuss.net/6/2911/2009/

Ocean Science Discussions

Short-term impacts of enhanced Greenland freshwater fluxes in an eddy-permitting ocean model

R. Marsh[1], D. Desbruyères[2], J. L. Bamber[3], B. A. de Cuevas[4], A. C. Coward[4], and Y. Aksenov[4]

[1]School of Ocean and Earth Science, University of Southampton, European Way, Southampton, Hampshire SO14 3ZH, UK
[2]Laboratoire de Physique des Océans, Université de Bretagne Occidentale, 6 av. Le Gorgeu CS 93837, 29238 Brest Cedex 3, France
[3]Bristol Glaciology Centre, School of Geographical Sciences, University of Bristol, UK
[4]National Oceanography Centre, Southampton (NOCS), European Way, Southampton, Hampshire SO14 3ZH, UK

Received: 11 November 2009 – Accepted: 16 November 2009
– Published: 27 November 2009

Correspondence to: R. Marsh (rma@noc.soton.ac.uk)

Published by Copernicus Publications on behalf of the European Geosciences Union.

Abstract

In a sensitivity experiment, an eddy-permitting ocean general circulation model is forced with freshwater fluxes from the Greenland Ice Sheet, averaged for the period 1991–2000. The fluxes are obtained with a mass balance model for the ice sheet, forced with the ERA-40 reanalysis dataset. The freshwater flux is distributed around Greenland as an additional term in prescribed runoff, representing seasonal melting of the ice sheet and a fixed year-round iceberg calving flux, for 8.5 model years. The impacts on regional hydrography and circulation are investigated by comparing the sensitivity experiment to a control experiment, without Greenland fluxes. By the end of the sensitivity experiment, the majority of additional fresh water has accumulated in Baffin Bay, and only a small fraction has reached the interior of the Labrador Sea, where winter mixed layer depth is sensitive to small changes in salinity. As a consequence, the impact on large-scale circulation is very slight. An indirect impact of strong freshening off the west coast of Greenland is a small anti-cyclonic circulation around Greenland which opposes the wind-driven cyclonic circulation and reduces net southward flow through the Canadian Archipelago by ~10%. Implications for the post-2000 acceleration of Greenland mass loss are discussed.

1 Introduction

The Greenland Ice Sheet (GrIS) appears to have been losing mass since the 1990s (van den Broeke et al., 2009). Over each annual cycle, this net mass loss comprises roughly equal amounts of surface runoff and solid ice fluxes across the grounding lines of ocean-terminating glaciers. Surface mass balance models of the GrIS provide the detailed pattern of runoff to the ocean (e.g., Fettweis, 2007). These data can be combined with estimates of grounding line fluxes from satellite observations of velocity (Rignot and Kanagaratnam, 2006) to produce the spatial distribution of freshwater fluxes (FWF), which can be prescribed as forcing in an ocean circulation model. Such an experiment has been undertaken using rough estimates of FWF from Greenland and Antarctica in a global model with 1° resolution (Stammer, 2008). That study suggested that advection of freshwater from the North Atlantic takes decades and is modulated by Rossby waves. As a result, there is an accumulation of freshwater that results in a substantial sea surface height (SSH) anomaly. The model resolution in that study was, however, insufficient to permit eddies and model boundary currents are broader than in reality.

Determining the precise fate of FWF from Greenland requires ideally an eddy-resolving model, as much of the flux may be entrained in the narrow boundary current that flows south along the east coast as the East Greenland Coastal Current (Bacon et al., 2002) and north along the west coast of Greenland, before returning south along the Canadian Arctic coast. If this is the case, then models that poorly resolve boundary currents may not be suitable for studying the impact of FWF on North Atlantic waters. To go some way to address this issue we employ an eddy-permitting model to explore the short-term advection and mixing of FWF from the GrIS. In comparing a meltwater-forced simulation to a control simulation, we effectively investigate the short-term impact of a sudden, sustained and substantial increase of GrIS meltwater input to the adjacent oceans. Investigation of this first-order impact is motivated by the recent acceleration in GrIS mass loss (Velicogna, 2009), and the likelihood that this melting will be sustained.

The paper is organized as follows. By way of experimental design, we outline the ocean model, and the method by which the freshwater fluxes are obtained and prescribed in the model. In the results section, we focus on the development of a fresh anomaly around Greenland, the impacts on regional hydrography, and associated changes in ocean circulation around Greenland. In the discussion, we draw some basic conclusions about the likely pattern of freshening that may soon be detected around Greenland. Caveats inherent in the present experimental design are also considered.

2 Experimental design

2.1 Ocean model

For the present experiments, we use an ocean model based on NEMO, the Nucleus for European Modelling of the Ocean. NEMO is a European modelling community effort to advance ocean modelling for the ocean climate research and operational oceanography through a state-of-art common flexible modelling framework. The core of the framework contains the ocean model OPA v9.0 and sea ice model LIM3. The LIM3 model is based on Elastic-Viscous-Plastic ice dynamics, has energy conserving thermodynamics, a multi-category representation of sea ice thickness and an explicit description of the salt evolution within sea ice. The last of these is essential in order to simulate sea ice evolution and sea ice-ocean coupling correctly (Vancoppenolle et al., 2009). Following Campin et al. (2008), we use the embedded sea ice scheme with a rescaled vertical coordinate for the sea ice-ocean coupling, for more accurate simulation of the mass and salt exchange between sea ice and ocean.

The NOCS version of NEMO is a global implementation at $1/4^{\circ}$ resolution (ORCA025). Due to the use of a curvilinear grid, ORCA025 has horizontal resolution of around 16 km in the vicinity of Greenland and the Labrador Sea. Figure 1 summarizes the statistics of surface current speed in the subpolar North Atlantic, for the NEMO control experiment. The left and right panels show the mean and standard deviation of surface current, respectively, for the period 1994–2001 over which we apply Greenland meltwater fluxes. The mean circulation is characterized by narrow (100–200 km width) boundary currents around the subpolar gyre, with maximum speeds of around 40 cm s^{-1} off Labrador and south Greenland. Standard deviation of current speed is typically an order of magnitude smaller than mean current speed, with the exception of higher standard deviations in the strongly-eddying North Atlantic Current. The NOCS configuration of NEMO also has an increased number of vertical levels, from 46 levels in the reference version to 64 levels, with a resolution of 6 m near the surface. This improves the simulation of sea ice and upper ocean dynamics.

The model is forced by the DFS3 set of surface fluxes, developed through the DRAKKAR consortium to drive the ORCA025-NEMO system and maintain a realistic overturning circulation in the Atlantic. Using this configuration of NEMO, a series of control experiments have been carried out for the period 1958–2001 (Grist et al., 2009). In the present study, additional GrIS freshwater fluxes are added from July 1993 onwards (to December 2001). The control and sensitivity experiments are directly compared, to identify the impact of GrIS fluxes on hydrography and circulation.

In addition to freshwater forcing, it is necessary to relax model surface salinity towards observed sea surface salinity (monthly-mean climatological values), in order to maintain a realistic overturning circulation. For the ice-free ocean, the relaxation coefficient is equivalent to a freshwater flux of 0.033 $\mathrm{m\,d^{-1}}$ per psu of salinity difference. In the presence of ice, much stronger relaxation is necessary, with a coefficient of 0.167 $\mathrm{m\,d^{-1}}$ per psu difference. This relaxation substantially reduces the actual additional GrIS freshwater fluxes that are imposed in the sensitivity experiment.

2.2 Climatological GrIS meltwater fluxes, 1991–2000

Ice sheet model estimates of seasonal surface runoff were obtained by forcing a high-resolution (5 km) mass balance model of the GrIS with ERA-40 surface boundary conditions for 1991–2000 (Bougamont et al., 2005). Monthly-mean melt-water fluxes were calculated for 1991–2000 and integrated downslope to produce surface runoff estimates at the ice margins. The solid ice fluxes were taken from published estimates derived from satellite velocity and ice thickness measurements, using the 1996 flux values (Rignot and Kanagaratnam, 2006). The total annual flux from the GrIS to the surrounding ocean, from this analysis, was 658 $\mathrm{km^3}$ compared with a mean accumulation over the ice sheet of 621 $\mathrm{km^3}$ for the same time period. The mass imbalance, of 37 $\mathrm{km^3\,yr^{-1}}$, is somewhat smaller than, but comparable in magnitude to, the estimate of the mass balance for 1996 from mass budget calculations (Rignot and Kanagaratnam, 2006). Due to strong relaxation of surface salinity in NEMO, the actual annual freshwater gain is considerably less than 658 $\mathrm{km^3\,yr^{-1}}$, actually averaging around 100 $\mathrm{km^3\,yr^{-1}}$

over 1993–2001.

The fluxes at individual gridcells within the GrIS were averaged up to the NEMO resolution and re-located at the nearest ocean gridcell, around the coast of Greenland, shown in Fig. 2. The pattern of FWF around the coastline of Greenland (also shown in Fig. 2) differ significantly from earlier, simpler, prescriptions (Saenko et al., 2007; Stammer, 2007), in which the strongest fluxes are located along the east coast. In the present study, the strongest fluxes are located along the west coast. The difference may be attributed to the period (1991–2000), while the other studies have speculated on the coastal distribution of more recent and future melting. Figure 3 shows monthly and annual-mean total runoff from Greenland coast for 1991–2000, revealing a strong seasonal cycle, with summer/autumn fluxes higher by O(10) compared to winter/spring fluxes. While there is some interannual variability in summer melt rates, we use monthly mean fluxes in the present experiment. Figure 4 shows the seasonal cycles of GrIS runoff specified in each year of the control and sensitivity experiments. In the sensitivity experiment, the additional GrIS fluxes boost total annual runoff from Greenland by a factor ranging from ∼2 (winter) to ∼4 (summer).

3 Results

On the short timescale considered here, and under modest additional freshwater forcing, the impact on large-scale circulation (subpolar gyre, meridional overturning) is almost indiscernible. We therefore focus on the immediate impact of freshwater addition on hydrography and circulation near to Greenland.

3.1 Impacts on hydrography and mixed layer depth

Over a timescale of 6 months, strong inputs of freshwater from southwest Greenland initially remain within 100–200 km of the coast, with more extensive offshore anomalies appearing in surface salinity off the west coast, in the vicinity of Davis Strait, just north of Disko Bugt, and just south of Nares Strait (Fig. 5). Over the subsequent 8 yr, more extensive annual-mean anomalies arise, notably to the west of Greenland (Fig. 6). Away from eddying regions, anomalies of sea surface temperature (SST) in the range ±0.5°C are confined to the boundary currents, with cooling off southern Greenland and warming off Labrador (Fig. 7). The contour ranges in Figs. 6 and 7 are chosen such that the minimum (maximum) of salinity (temperature) change corresponds to the same reduction in surface density, indicating the relative influence on stratification of changes in surface salinity and temperature. Strongest annual-mean warming off Labrador arises in 1997 and 1998, and is coincident with locally increased surface salinity (see Fig. 6). This may be associated with increased winter mixed layer depth in the northern Labrador Sea (see Fig. 9) which enhances the upward mixing of relatively warm and saline water that lies immediately beneath the cold, fresh surface layer. Large positive and negative anomalies of salinity and tempertaure arise in the inter-gyre zone, due to remote disturbance of the strongly-eddying North Atlantic Current, akin to the "butterfly effect" describing the sensitivity of weather forecasts to small perturbations of initial conditions.

Sub-surface salinity anomalies develop and spread over the sensitivity experiment, but strong anomalies (exceeding ±0.2 psu) are confined to the upper 200 m. Figure 8 illustrates the evolution of salinity anomalies at 106 m, a depth level representative of this freshening layer. The pattern is dominated by the development of negative anomalies in Baffin Bay, where relatively weak circulation and a degree of recirculation is presumed to increase the residence time for enhanced GrIS runoff. The development of substantial salinity anomalies in the Arctic, off the north coast of Greenland, is less obviously explained, as runoff is not locally enhanced (see Fig. 2). This fresh signal is perhaps due to a reduction in Arctic freshwater export, linked to a change in the flows east and west of Greenland (see Sect. 3.2).

End-of-winter (March) mixed layer depth (MLD) in the Labrador Sea is rather sensitive to the additional melt water, deepening and shoaling by more than 500 m in some locations (Fig. 9), although these large anomalies are associated with deep mixed lay-

OSD
6, 2911–2937, 2009

ers in the same locations (Fig. 10). Some areas of deepening persist throughout (e.g., at the northern rim of the Labrador Sea) and shoaling adjacent to most of the Labrador Current is persistent after 1997. Elsewhere, there is considerable spatial and interannual variability. In spite of this change in MLD, there is little discernible influence on the meridional overturning circulation (not shown).

3.2 Changes in freshwater and heat content, sea level and regional circulation

We consider changes in integral quantities between early and later stages of the experiment, in 1995 and 2001, respectively. While the sub-surface spreading of a fresh anomaly is largely restricted to the upper 200 m, freshwater content increases substantially across the region, evident as horizontally-spreading negative salt content anomalies (Fig. 11a, upper panels). Patterns of salt content anomaly are similar to salinity anomaly at 106 m (see Fig. 8). By 2001, the majority of additional freshwater added over 1993–2001 has accumulated in Baffin Bay, with less prominent anomalies off the southeast coast of Greenland and in the Arctic Ocean adjacent to northern Greenland. Although an anomalous fresh signal can be traced along the narrow boundary current of the Labrador Sea, relatively little additional freshwater reaches the interior of the subpolar gyre, where only small negative anomalies develop by 2001. Corresponding heat content anomalies (Fig. 11b, middle panels) indicate relatively smaller indirect impacts on temperature throughout the water column, notably in Baffin Bay, where salt content anomalies can be expected to dominate local density changes.

As a consequence of freshwater gain, depth-averaged density is reduced, the water column expands, and sea surface height (SSH) increases sterically. The pattern of annual-mean SSH differences between the two experiments (Fig. 11c, lower panels) confirms that SSH increases around Greenland, by up to 5 cm in Baffin Bay, coincident to a large extent with increased freshwater content. The direct effect on sea level of a mass influx associated with runoff is not included in NEMO, so the SSH changes in Fig. 11c are the combination of steric effects (due to changes of both salinity and temperature) and changes in bottom pressure associated with the barotropic mode of circulation.

A notable feature in Fig. 11c is the ~2 cm increase of coastal SSH around Greenland. This suggests a re-adjustment of the round-island circulation explained by Godfrey's Island Rule (Godfrey, 1989), which was recently shown to apply for Greenland (Joyce and Proshutinsky, 2007). While Godfrey's Island Rule was formulated for wind-driven barotropic circulations, buoyancy forcing – in the present case, strong runoff – can also force a barotropic flow in the vicinity of a shelf break via the Joint Effect of Baroclinicity And Relief (JEBAR, see Huthnance, 1984). Indeed, JEBAR has been invoked to explain an observed seasonal cycle in the inshore Labrador Current (Lazier and Wright, 1993): shelf-break transport is observed to peak in October after reaching minimum values in March–April, a seasonal variation that has been associated with the flux of freshwater onto the shelf during summer. SSH rise around Greenland is consistent with fast boundary wave propagation, observed throughout the World Ocean (Hughes and Meredith, 2006). An anomalous SSH signal originating principally in Baffin Bay would propagate around Greenland as a coastally-trapped wave with a phase speed of several $\mathrm{m\,s^{-1}}$. With a coastline of ~40 000 km, boundary waves travelling at a speed of $5\,\mathrm{m\,s^{-1}}$ would complete a circuit of Greenland in around 90 days to establish a perturbed round-island flow.

The evidence for such a perturbed flow is provided by a comparison of the southward transport west of Greenland in the two experiments (Fig. 12). When Greenland melting is included, southward transport in Davis Strait (capturing nearly all of the west Greenland flow) is reduced by around 10% (e.g., from 2.45 Sv to 2.22 Sv in 2001). Based on a simple geostropic balance, reduction in transport of 0.23 Sv is consistent with the corresponding change in cross-shelf slope of sea surface height (Fig. 11c). At 70° N, an anomalous slope (up towards the coast) of 2 cm across a shelf of typical width 200 km yields an anomalous depth-averaged velocity of $0.7\,\mathrm{cm\,s^{-1}}$ (anti-cyclonic around Greenland). For a typical shelf depth of 200 m (and width 200 km), this correponds to a reduction in southward transport (west of Greenland) of 0.29 Sv. The interannual variability evident in Fig. 12 (both runs) is most likely driven by changes in wind forcing (identical in both model runs). We infer that an indirect impact of the strongest freshening off the west coast of Greenland is a small anti-cyclonic (clockwise) round-Greenland flow, opposing the cyclonic wind-driven circulation and associated southward flow through the Canadian Archipelago.

4 Discussion

The main conclusions drawn from this study are as follows:

1. Over a timescale of 6 months, strong inputs of freshwater from southwest Greenland initially remain within 100–200 km of the coast.
2. Over a timescale of eight years, an anomalous fresh signal can be traced along the narrow boundary current of the Labrador Sea, but the majority of additional freshwater added over 1993–2001 accumulates in Baffin Bay.
3. Comparisons of imposed and actual global freshwater content anomaly indicate that net freshening amounts to ∼15% of the imposed freshening, due to strong surface salinity relaxation in the model used here.
4. As a consequence of (2), relatively little additional freshwater reaches the interior of the subpolar gyre, and impacts on mixed layer depth and convection are limited.
5. On the short timescale considered here, and under modest additional freshwater forcing, the impact on large-scale circulation is almost indiscernible, although strong freshening along the west coast of Greenland leads to reduction by ∼10% in the cyclonic flow around Greenland (and associated Arctic export west of Greenland).

The extent to which a fresh anomaly builds up year on year depends in part on the efficiency with which the surface anomaly is mixed vertically into the water column,

OSD
6, 2911–2937, 2009

Title Page
Abstract Introduction
Conclusions References
Tables Figures
◀◀ ▶▶
◀ ▶
Back Close
Full Screen / Esc
Printer-friendly Version
Interactive Discussion

while anomalies remaining at the surface are more effectively damped through relaxation towards observed surface salinity. While extra freshwater is added at a rate of 658 $km^3 yr^{-1}$, the overall, long-term effect of relaxation is therefore to effectively reduce this influx, most efficiently in the presence of sea ice. Over 1993–2001, freshwater is actually gained at a much lower rate of around 100 $km^3 yr^{-1}$, which is close to recent estimates for the enhanced rate of Greenland mass loss (Box et al., 2004; Velicogna and Wahr, 2006; IPCC, 2007). The experiment hence serves as a useful guide to the pathways of the additional freshwater entering the boundary currents around Greenland during and since the 1990s.

Given the dominance of freshwater accumulation in Baffin Bay, we consider observational evidence for regional freshening that may be a signature of GrIS melting. Hydrographic observations in Baffin Bay are relatively sparse. Although such observations are sufficient to discern long-term warming and freshening (Zweng and Münchow, 2006), little information is available on recent salinity changes. We note, however, that the strongest long-term freshening has occurred in the upper 250 m on the west Greenland and Baffin Island shelf breaks (see Figs. 8 and 9 in Zweng and Münchow, 2006). While these trends may be associated with changes in the strength and properties of waters exchanged with the Arctic and the Labrador Sea, our simulation supports an alternative possibility that GrIS meltwater may contribute to the freshening in these locations. With little knowledge of GrIS changes prior to 1990, it is not possible to further substantiate this. As simulated here, the relatively weak signal of Greenland melting in local boundary currents will be difficult to detect from hydrographic data. While it is now possible to identify Greenland melt water in hydrographic measurements in sections running up to the Greenland coast, signals of change are still within the errors and uncertainties inherent in such a freshwater budget (Sutherland and Pickart, 2008).

An intriguing result is that the additional melting of Greenland has impacted on the primarily wind-driven cyclonic circulation around Greenland (Joyce and Proshutinsky, 2007). In the present experiment, the additional runoff lowers salinity throughout the water column around Greenland, which raises sea surface height (SSH) by ~2 cm due to the steric effect of freshening and we infer a weak buoyancy-driven cyclonic circulation that reduces the round-island flow by ~10%. This effect should be included alongside the direct effect of mass-flux on SSH and round-island flow, which is not included in NEMO. For completeness, we estimate here the latter effect. Taking a mean annual influx of 0.01 Sv (annual addition of 3.15×10^{11} m^3), spread over an average 200 km of shelf extending from the coast of Greenland (coastline length ~40 000 km, hence shelf area 8×10^{12} m^2), sea level would be raised by ~4 cm. This is additional to (in the same sense as) the steric effect on SSH, so assuming a similar, additional, dynamic response, the round-island flow would be reduced by a further 20%. As a consequence, the southward flow west of Greenland may in total be reduced by a third. Whether melting-related changes in flow west of Greenland can be detected will depend on the extent to which we can account for the larger variability due to changes of wind forcing associated with the Arctic Oscillation in particular (Joyce and Proshutinsky, 2007).

Non-eustatic changes in sea level occur when ice sheets melt due, primarily, to changes in the gravity field (Mitrovica et al., 2001). These changes result in a lowering in the near field of the ice sheet and rise in the far field. Attempts have been made to use this pattern of sea level changes as a "fingerprint" for the contribution of different ice masses to sea level (Mitrovica et al., 2001). The effect of FWF on ocean dynamics may, however, be the dominant signal on sea level rather than the gravity (Stammer, 2008). Here, we also find that the short-term local effect on sea level clearly exceeds the larger-scale gravitational effects. After 8 yr, the SSH anomaly (Fig. 11c) lies in the range ±5 cm in the Labrador and Irminger Seas, with large variability at the scale of eddies. For comparison, the implied net FWF gain in NEMO of 100 km^3 yr^{-1} is equivalent to an eustatic rise in global sea level of 0.3 mm yr^{-1}.

In summary, we have forced a state-of-the-art eddy-permitting global ocean model with realistic freshwater fluxes from the Greenland Ice Sheet. The freshwater fluxes are in turn obtained by forcing a mass balance ice sheet model for the period 1991–2000. The ocean model is forced with the 1991–2000 monthly-mean fluxes from summer 1993 onwards, and the simulated freshening thereafter is evident by comparison with a control experiment in which no additional freshwater forcing is imposed. Implicit in this experimental approach is the simple assumption that freshwater input from the Greenland Ice Sheet can change in one year and thereafter remain constant. While our design is admittedly somewhat idealized, the experiment is a first step towards understanding the fate of additional Greenland melt water and ice in the presence of narrow boundary currents and eddies. Only at sufficiently high resolution are these features explicitly resolved. However, the very narrow (width scale 30 km) East Greenland Coastal Current, considered to act as a conduit for Greenland melt water along the east coast (Bacon et al., 2002; Sutherland and Pickart, 2008), is unresolved in the $1/4^{\circ}$ version of NEMO used in the present study.

The experiment provides a basis for further studies. With an improving knowledge of recent changes in the Greenland mass loss, and more up-to-date boundary conditions for forcing NEMO through these more recent years, we can soon extend new experiments to investigate the extent to which actual changes in the ice sheet are freshening the ocean and seas around Greenland. Further prospects include explicit representation of the iceberg flux and along-trajectory melting (Bigg et al., 1997; Jongma et al., 2008; Levine and Bigg, 2008). An outstanding challenge is the representation of non-hydrostatic effects associated with the substantial mass influx, and hence the full implications for barotropic flow around Greenland and Arctic export through the Canadian Archipelago.

Acknowledgements. This study was originally undertaken as an MSc project at the University of Southampton by D. Desbruyères. The development, use and analysis of NEMO are funded through the "Oceans 2025" Strategic Research Programme of the UK Natural Environment Research Council (NERC), which also supports the research of A. Coward, B. de Cuevas and Y. Aksenov. JLB was funded by UK NERC grants NER/T/S/2002/00462 and NE/C509474/1.

References

Bacon, S., Reverdin, G., Rigor, I. G., and Snaith, H. M.: A freshwater jet on the east Greenland Shelf, J. Geophys. Res., 107(C7), 1–5, doi:10.1029/2001JC000935, 2002.

Bigg, G. R., Wadley, M. R., Stevens, D. P., and Johnson, J. A.: Modelling the dynamics and thermodynamics of icebergs, Cold Reg. Sci. Technol., 26, 113–135, 1997.

Bougamont, M., Bamber, J. L., and Greuell, W.: A surface mass balance model for the Greenland Ice Sheet, J. Geophys. Res., 110, F04018, doi:10.1029/2005JF000348, 2005.

Box, J. E., Bromwich, D. H., and Bai, L.-S.: Greenland Ice Sheet surface mass balance 1991–2000: application of polar MM5 mesoscale model and in situ data, J. Geophys. Res., 109, D16105, doi:10.1029/2003JD004451, 2004.

Campin, J. M., Marshall, J., and Ferreira, D.: Sea-ice ocean coupling using a rescaled vertical coordinate z*, Ocean Model., 24, 1–14, 2008.

Fettweis, X.: Reconstruction of the 1979–2006 Greenland Ice Sheet surface mass balance using the regional climate model MAR, Cryosphere, 1, 21–40, 2007.

Godfrey, J. S.: A Sverdrup model of the depth-integrated flow from the world ocean allowing for island circulations, Geophys. Astro. Fluid, 45, 89–112, 1989.

Grist, J. P., Josey, S. A., Marsh, R., Good, S., Coward, A. C., deCuevas, B. A., Alderson, S. G., New, A. L., and Madec, G.: The roles of surface heat flux and ocean heat transport during four decades of Atlantic Ocean temperature variability, Ocean Dynam., submitted, 2009.

Hughes, C. W. and Meredith, M. P.: Coherent sea-level fluctuations along the global continental slope, Philos. T. R. Soc. Lond., 364, 885–901, 2006.

Huthnance, J. M.: Slope currents and “JEBAR”, J. Phys. Oceanogr., 14, 795–810, 1984.

IPCC: WG1 AR4 Report, Chapt. 4, “Observations: Changes in Snow, Ice and Frozen Ground”, Sect 4.6, “Changes and Stability of Ice Sheets and Ice Shelves”, CUP, Cambridge, 996 pp., 2007.

Jongma, J. I., Driesschaert, E., Fichefet, T., Goosse, H., and Renssen, H.: Facilitation of Southern Ocean sea ice formation in a three dimensional climate model with interactively coupled icebergs, Ocean Model., 26, 104–113, 2008.

Joyce, T. M. and Proshutinsky, A.: Greenland's island rule and the Arctic Ocean circulation, J. Mar. Res., 65, 639–653, 2007.

Lazier, J. R. N. and Wright, D. G.: Annual velocity variations in the Labrador Current, J. Phys. Oceanogr., 23, 659–678, 1993.

Levine, R. C. and Bigg, G. R.: Sensitivity of the glacial ocean to Heinrich events from different iceberg sources, as modeled by a coupled atmosphere-iceberg-ocean model, Paleoceanography, 23, PA4213, doi:10.1029/2008PA001613, 2008.

Mitrovica, J. X., Tamisiea, M. E., Davis, J. L., and Milne, G. A.: Recent mass balance of polar ice sheets inferred from patterns of global sea-level change, Nature, 409(6823), 1026–1029, 2001.

Rignot, E. and Kanagaratnam, P.: Changes in the velocity structure of the Greenland Ice Sheet, Science, 311(5763), 986–990, 2006.

Saenko, O. A., Weaver, A. J., Robitaille, D. Y., and Flato, G. M.: Warming of the subpolar Atlantic triggered by freshwater discharge at the continental boundary, Geophys. Res. Lett., 34, L15604, doi:10.1029/2007GL030674, 2007.

Stammer, D.: Response of the global ocean to Greenland and Antarctic ice melting, J. Geophys. Res., 113, C06022, doi:10.1029/2006JC004079, 2008.

Sutherland, D. and Pickart, R. S.: The East Greenland Coastal Current: structure, variability, and forcing, Prog. Oceanogr., 78, 58–77, 2008.

Vancoppenolle, M., Fichefet, T., Goosse, H., Bouillon, S., Madec, G., and Morales Maqueda, M. A.: Simulating the mass balance and salinity of Arctic and Antarctic sea ice. 1. Model description and validation, Ocean Model., 27, 33–53, doi:10.1016/j.ocemod.2008.10.005, 2009.

van den Broeke, M., Bamber, J. L., Ettema, J., Rignot, E., Schrama, E. J. O., van de Berg, W., van Meijgaard, E., Velicogna, I., and Wouters, B.: Partitioning recent Greenland mass loss, Science, 326, 984–986, 2009.

Velicogna, I. and Wahr, J.: Acceleration of Greenland ice mass loss in spring 2004, Nature, 443, 329–331, 2006.

Velicogna, I.: Increasing rates of ice mass loss from the Greenland and Antarctic Ice Sheets revealed by GRACE, Geophys. Res. Lett., 36, L19503, doi:10.1029/2009GL040222, 2009.

Zweng, M. M. and Münchow, A.: Warming and freshening of Baffin Bay, 1916–2003, J. Geophys. Res., 111, C07016, doi:10.1029/2005JC003093, 2006.

OSD

6, 2911–2937, 2009

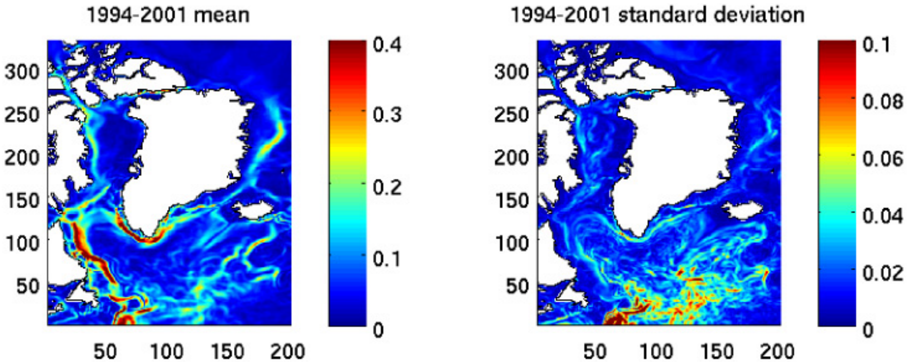

Fig. 1. Surface current speed in the NEMO control experiment: mean (left panel) and standard deviation (right panel), for 1994–2001.

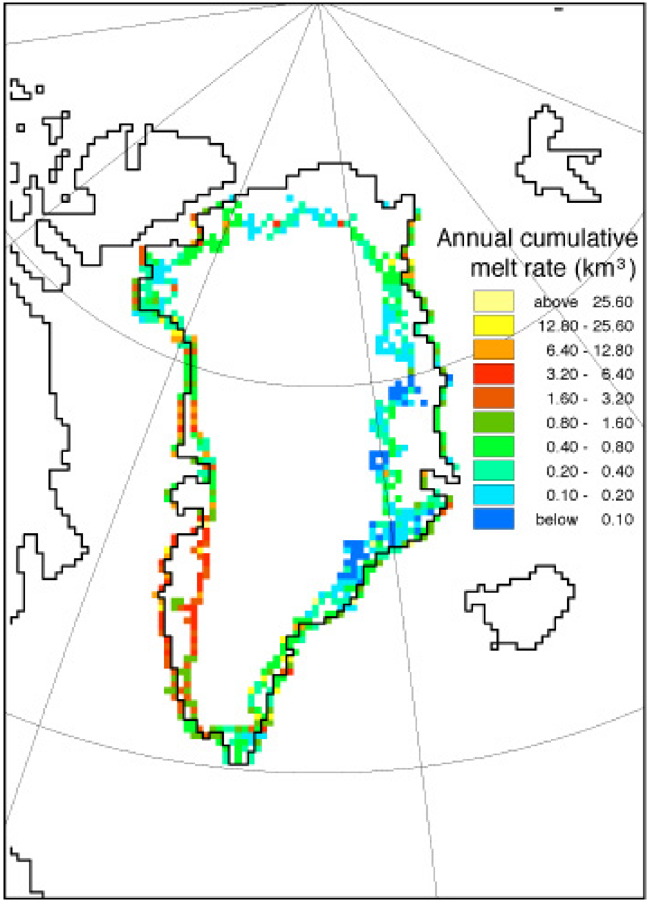

Fig. 2. Annual melt fluxes (km^3) predicted with an energy mass balance model of the Greenland Ice Sheet (averaged for 1991–1999), as located on the ice sheet and re-located to coastal gridcells.

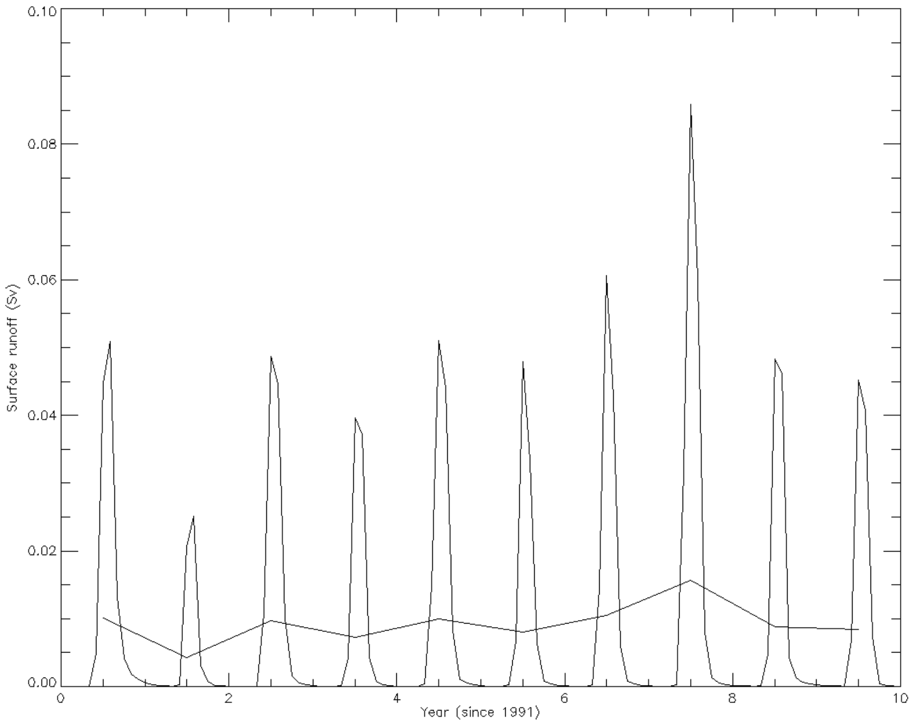

Fig. 3. Monthly and annual-mean surface runoff (Sv) from Greenland for 1991–1999. This does not include the iceberg calving fluxes, which are assumed constant throughout the year. The iceberg flux is approximately equal in magnitude to the mean annual runoff in the simulation.

OSD

6, 2911–2937, 2009

Title Page
Abstract
Introduction
Conclusions
References
Tables
Figures
◄
►
Back
Close
Full Screen / Esc
Printer-friendly Version
Interactive Discussion

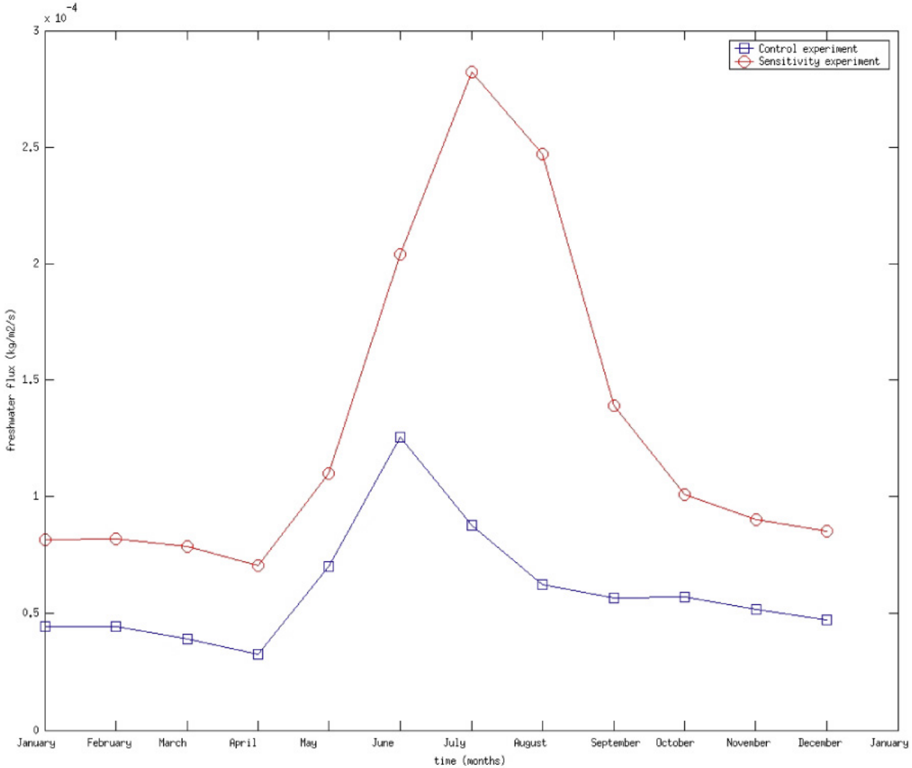

Fig. 4. Seasonal cycles of surface runoff (freshwater forcing, $\mathrm{kg\,m^{-2}\,s^{-1}}$) along the Greenland coast, for the control experiment (blue curve) and the sensitivity experiment (red curve).

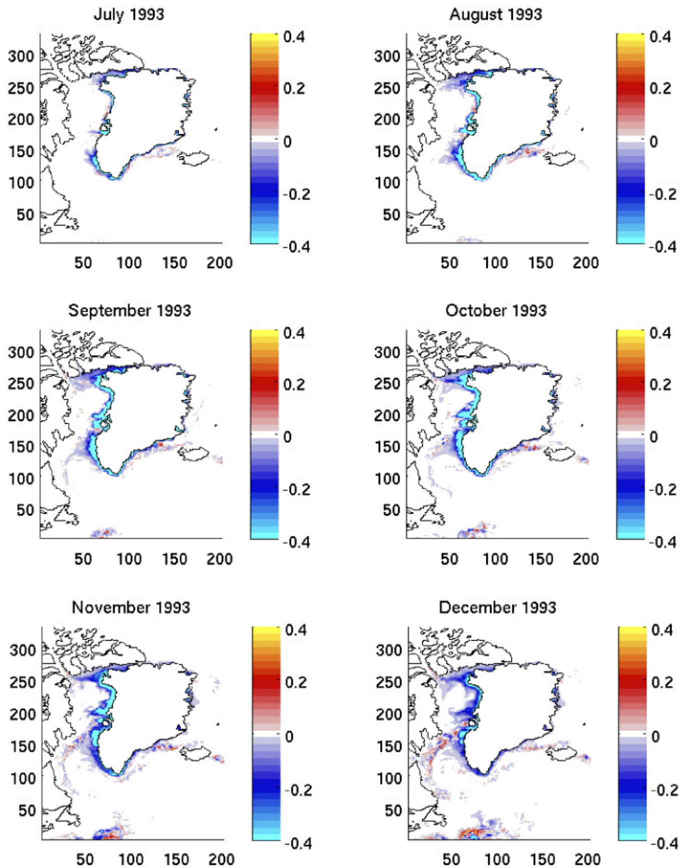

Fig. 5. Monthly anomalies of sea surface salinity (psu) around Greenland for the period July 1993–December 1993. These and subsequent anomalies are obtained as "sensitivity minus control" differences.

OSD
6, 2911–2937, 2009

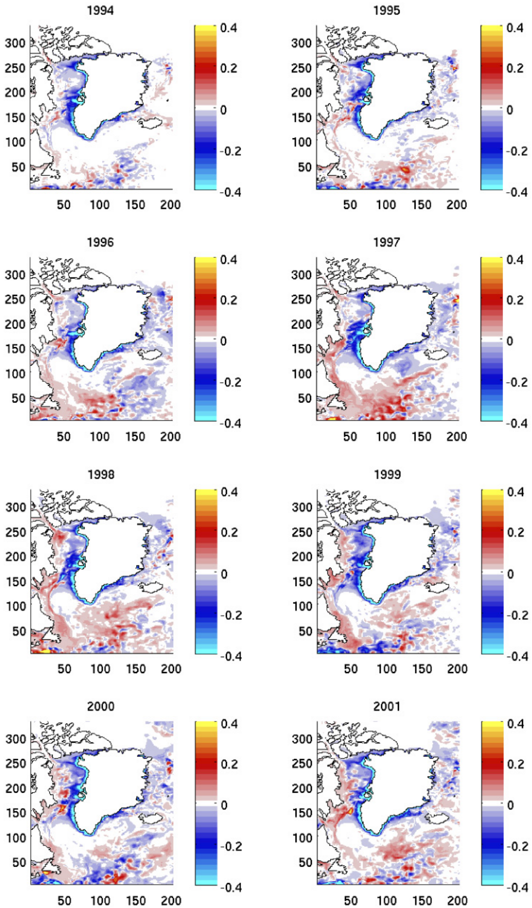

Fig. 6. Annual mean surface salinity anomalies (psu) for the period 1994–2001.

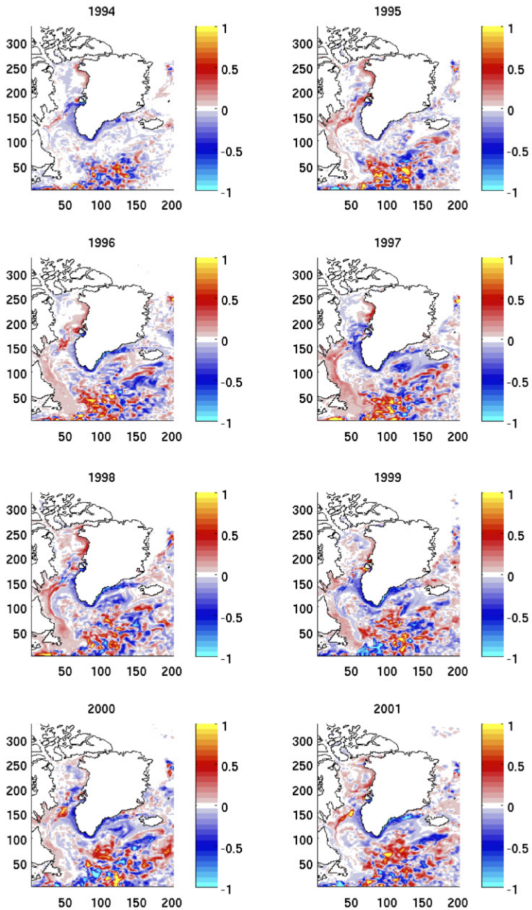

Fig. 7. Annual mean sea surface temperature anomalies (˚C) for the period 1994–2001.

OSD
6, 2911–2937, 2009

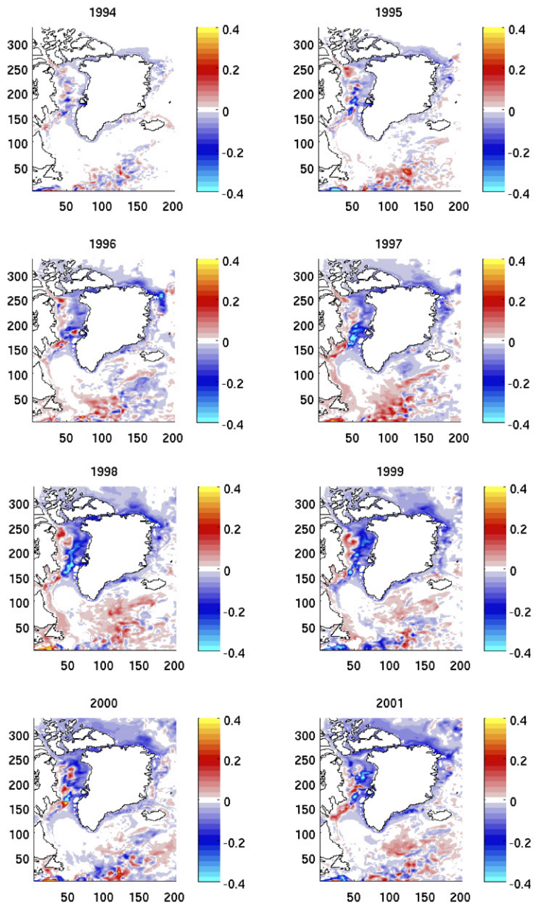

Fig. 8. Annual mean 106 m salinity anomalies (psu) for the period 1994–2001.

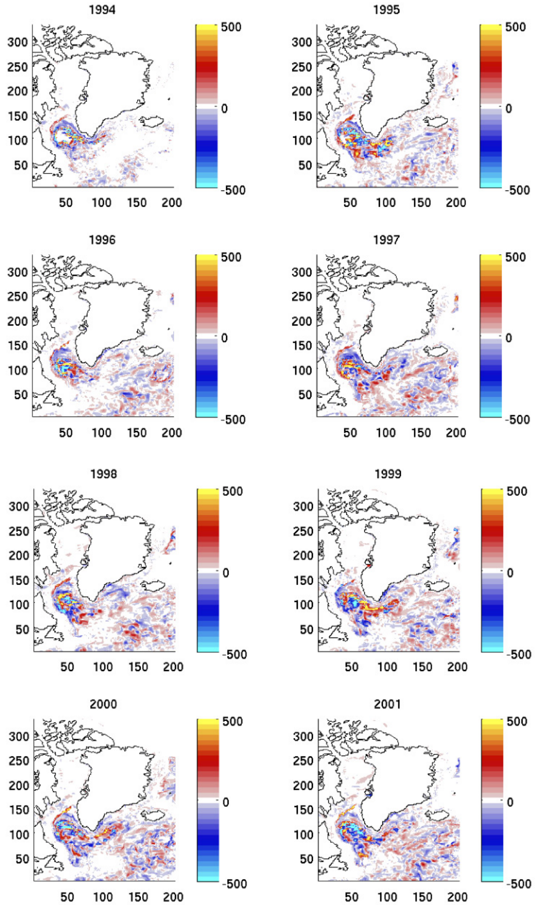

Fig. 9. March mixed layer depth anomalies (m) for the period 1994–2001.

OSD
6, 2911–2937, 2009

Title Page
Abstract Introduction
Conclusions References
Tables Figures
Back Close
Full Screen / Esc
Printer-friendly Version
Interactive Discussion

OSD
6, 2911–2937, 2009

Greenland freshwater

R. Marsh et al.

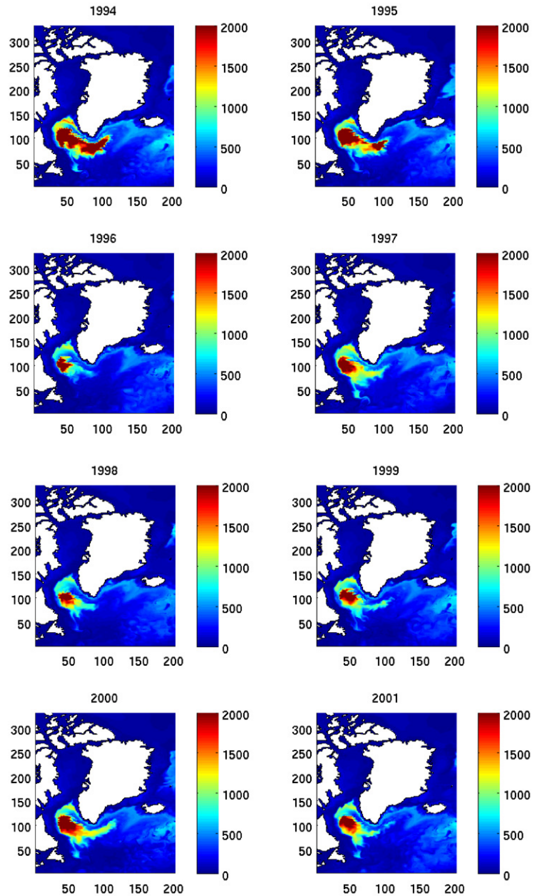

Fig. 10. March mixed layer depth (m) for the period 1994–2001 in the control experiment.

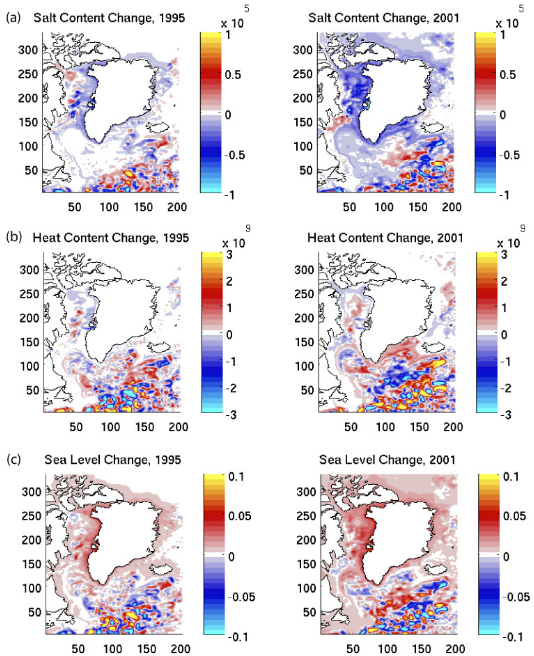

Fig. 11. Annual-mean differences ("sensitivity minus control"), in 1995 and 2001: **(a)** Salt content ($\mathrm{kg\,m^{-3}}$); **(b)** Heat content ($\mathrm{J\,m^{-2}}$); **(c)** Sea surface height (m).

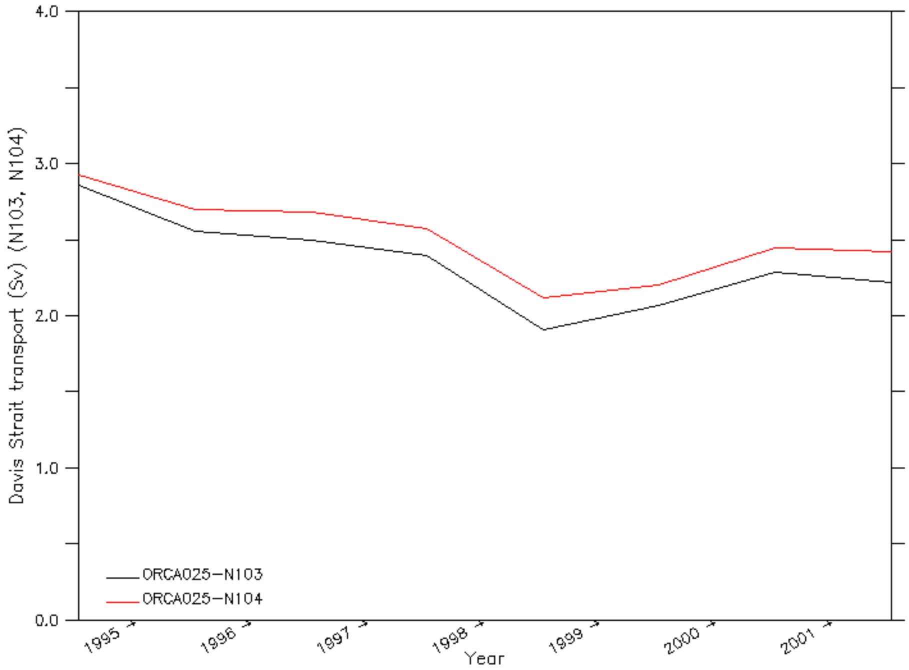

Fig. 12. Annual-mean southward volume transport in Davis Strait (Sv, positive southward) over 1995–2001, in control experiment (ORCA025-N104, red curve) and sensitivity experiment (ORCA025-N103, black curve).

OSD
6, 2911–2937, 2009

Title Page
Abstract Introduction
Conclusions References
Tables Figures
Back Close
Full Screen / Esc
Printer-friendly Version
Interactive Discussion